

**MARINER 9 ULTRAVIOLET SPECTROMETER EXPERIMENT:  
INTERSTELLAR ABSORPTION AT LYMAN ALPHA  
IN OB STARS**

RALPH C. BOHLIN

Department of Astro-Geophysics and Laboratory for Atmospheric and Space Physics,  
University of Colorado, Boulder

*Received 1972 November 27*

**ABSTRACT**

Column densities of neutral hydrogen  $N_{\text{H}}$  toward 10 stars are derived from spectra obtained with the ultraviolet spectrometer (UVS) on the *Mariner 9* Mars orbiter. The 7.5 Å resolution is sufficient for a direct analysis of the data without assumptions about the strength of the lines that blend with the  $L\alpha$  profile at lower resolution. The deduced values of  $N_{\text{H}}$  are systematically lower than those derived from OAO-2 data.

*Subject headings:* abundances — early-type stars — interstellar matter — spectra, ultraviolet

**I. INTRODUCTION**

Early rocket observations of interstellar absorption at  $L\alpha$  in the spectra of early-type stars indicated that the density of neutral hydrogen  $n_{\text{H}}$  was about a factor of 7 lower than that expected from 21-cm measurements for 14 of 18 stars observed (Jenkins 1970, 1971). Values of  $n_{\text{H}} \approx 0.7 \text{ cm}^{-3}$  in the galactic plane are usually obtained from 21-cm emission measures (Kerr and Westerhout 1965). In retrospect, observational selection seems to have caused most of the disagreement, because 12 of the 14 stars, including nine in Orion, were between galactic longitudes  $180^\circ$  and  $270^\circ$  where there does appear to be an actual deficiency of gas. Kovach (1972) suggested that the 21-cm emission measures in Orion are still nearly normal because of an enhancement of the 21-cm transition probability for hydrogen atoms on charged grains. Recent analysis for a larger set of ultraviolet spectra produced better agreement with other measurements of neutral hydrogen. From OAO-2 scans of  $L\alpha$  for 69 stars, Savage and Jenkins (1972, hereafter referred to as SJ) found a mean density of  $0.6 \text{ atoms cm}^{-3}$ , but for the seven stars closer than 140 pc  $n_{\text{H}}$  was only  $0.25 \text{ atoms cm}^{-3}$ . The density for the closest stars is in agreement with the  $0.1\text{--}0.2 \text{ atoms cm}^{-3}$  found by Bertaux, Ammar, and Blamont (1972) in the immediate vicinity of the Sun. They obtained the density by modeling the intensity distribution of the scattered solar  $L\alpha$  emission from the sky-brightness maps of Thomas and Krassa (1971) and Bertaux and Blamont (1971).

If the results of SJ are correct, then the average densities found from  $L\alpha$  absorption and 21-cm emission are in good agreement, even though fluctuations on a scale smaller than the radio beamwidths may exist. Since the OAO-2 resolution (12 Å) is not sufficient to resolve the strong lines that lie near  $L\alpha$ , SJ compared the OAO data to synthetic stellar spectra derived from high-resolution rocket data which were processed to simulate absorption by different column densities of hydrogen and subsequent degradation of the resolution by the spectrometer. Because SJ used only eight rocket spectra as prototypes to determine  $N_{\text{H}}$  for the remainder of the stars, errors could arise from a mismatch in spectral types or from peculiarities of the individual stars. Independent data from *Mariner 9*, which has 7.5 Å resolution in second order, is analyzed directly to obtain  $N_{\text{H}}$  without use of prototype stars. Most of these values fall within the error bars of SJ, but small systematic reductions of the SJ results are indicated.

## II. OBSERVATIONS

The *Mariner 9* UVS (Pearce *et al.* 1971) is an Ebert-Fastie design with a telescope of only 29 cm<sup>2</sup> collecting aperture, almost a factor of 10 less than the OAO-2 scanner. However, long integration times of up to 2 hours per terrestrial day were available for astronomical observations (Lillie *et al.* 1972; Bohlin, Henry, and Swandic 1973). Since the limit cycle of the spacecraft attitude control system is  $\pm 0.25^\circ$ , a point source will remain in the 0.17 wide slit only about one-third of the time on the average. A signal at  $L\alpha$  from the Martian corona and sky background is always present. The shape of the  $L\alpha$  emission is the instrumental profile determined by the entrance and exit slit widths. This nonstellar contribution, measured when the limit cycle carries the star off the slit, can be precisely subtracted from the recorded spectra to produce a pure spectrum.

Two data channels record spectra covering the 1150–3400 Å region once every 3 seconds. The short-wavelength channel scans from the MgF cutoff at 1150 Å to the CsI limit of the photomultiplier near 2000 Å in first order and from 1150 to 1650 Å in second order. The full width at half-maximum of the triangular instrumental profile is 15 and 7.5 Å in first and second orders, respectively. Individual samples are recorded every 5 ms or about three times per resolution element.

The spectra presented in this paper were obtained between 1971 November 28 and 1972 February 17. All the scans made when a star was in the entrance slit were averaged for the daily observations of individual targets. The instrumental offset plus dark current was found near 2200 Å where the solar blind detector does not respond. This constant background and the  $L\alpha$  signal from the sky were removed, and the stellar spectrum was decalibrated to a relative flux scale. Because the stellar flux is fairly flat near  $L\alpha$ , it is not necessary to normalize the observations to the continuum. Finally, the data were smoothed with a sliding two-point average, so that every other point is totally independent. This smoothing was less than the resolution and did not significantly degrade the spectrum. The wavelength scale is usually accurate to  $\pm 1$  Å, although errors of about 2 Å are present in a few cases. The stellar observations were limited by two factors: the sensitivity of the detector and the area of the celestial sphere available to the scan platform.

## III. ANALYSIS

SJ note that the stellar  $L\alpha$  line is strong for spectral types B2.5 and later, but for types B2 and earlier interstellar absorption completely dominates the profile for  $N_{\text{H}} > 10^{20}$  atoms cm<sup>-2</sup>. Therefore, for these hottest stars the flux  $F$  is related to the continuum flux  $F_0$  by

$$F = F_0 \exp(-\tau), \quad (1)$$

where  $\tau$  is the optical depth through the interstellar gas given in terms of the wavelength  $\lambda$  in angstroms ( $\lambda_0 = 1215.67$  Å) by

$$\tau(\lambda) = 7.06 \times 10^{-11} N_{\text{H}} [1 + 1.66 \times 10^9 (\lambda - \lambda_0)^2]^{-1}. \quad (2)$$

$N_{\text{H}}$  has units atoms cm<sup>-2</sup>, and  $\tau$  is determined solely by the natural line profile, since radiation damping dominates all other forms of line broadening.

Smearing equation (1) with the instrumental profile and two-point smoothing generates line profiles  $F_s$  for different values of  $N_{\text{H}}$  that can be compared directly with the data. In addition to noise in the data, the two main problems in fitting the theoretical profiles  $F_s$  to the data are line blending and uncertain continuum levels  $F_0$ .

Line-blending problems are largely overcome by the 7.5 Å resolution in second order (fig. 1*a*). Direct analysis is virtually impossible at the 15 Å resolution of first

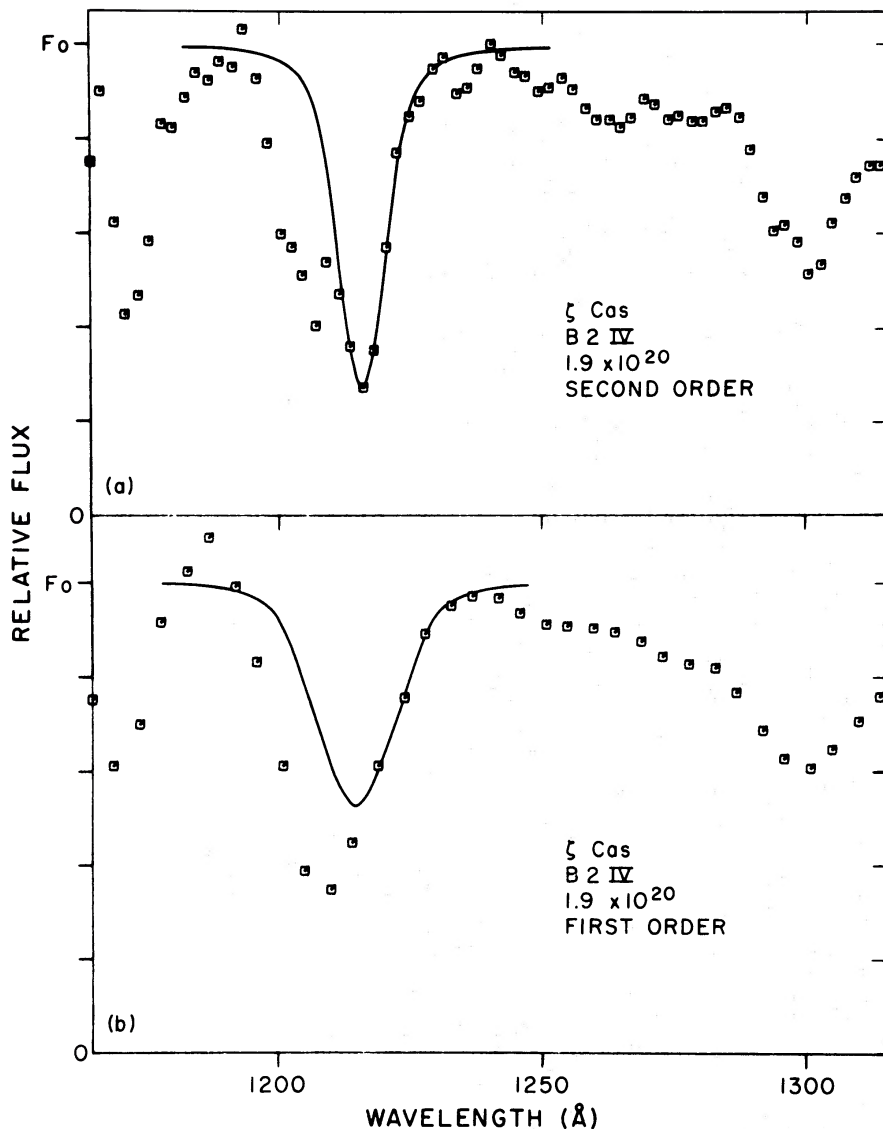


FIG. 1.—Spectra of  $\zeta$  Cas (B2 IV) in (a) second order with  $7.5 \text{ \AA}$  resolution and (b) first order with  $15 \text{ \AA}$  resolution. (a) The solid curve fitted to the  $L\alpha$  line is the damping profile for  $N_{\text{H}} = 1.9 \times 10^{20} \text{ atoms cm}^{-2}$  convolved with the instrumental profile for second order. (b) The same damping profile for first-order resolution is drawn in at the wavelength of  $L\alpha$ . Accurate values of  $N_{\text{H}}$  are difficult to obtain directly from the first-order data alone.

order (fig. 1b). For the star  $\zeta$  Cas (B2 IV) the main blending is due to the resonance line of Si III at  $1206.5 \text{ \AA}$ , which is strong in B2 stars. In the second-order spectrum, this line is partially resolved so that eight data points in the  $L\alpha$  profile are uncontaminated by Si III. A fit of  $F_s$  for  $N_{\text{H}} = 1.9 \times 10^{20} \text{ atoms cm}^{-2}$  is shown to pass through the resolved points. This procedure is successful in determining  $N_{\text{H}}$ , even though it is impossible to measure the equivalent width of  $L\alpha$  directly. A degraded profile for  $N_{\text{H}} = 1.9 \times 10^{20} \text{ atoms cm}^{-2}$  for first order is shown in figure 1b. Only three data points lie on the fit and are unaffected by the blending with Si III. In the presence of noise and small wavelength uncertainties,  $N_{\text{H}}$  cannot be derived from spectra with a resolution of  $\sim 15 \text{ \AA}$  without additional information.

Errors caused by misplacing the continuum  $F_0$  are largely eliminated by fitting theoretical profiles to the data points. The profile with the best fit overall is produced when the true value of  $F_0$  is used. For example, two curves for  $F_S (2.3 \times 10^{20} \text{ atoms cm}^{-2})$  with a difference of 10 percent in  $F_0$  are shown with the second order data for 15 Mon in figure 2. The upper curve is a better fit to the data in the wings, even though the central parts of the two profiles do not differ significantly. Thus, the information gained by knowing the necessary shape of the absorption and by using points over the whole profile determines both  $F_0$  and  $N_H$ , which depends only weakly on  $F_0$ .

The best-fit profiles to the second-order data for eight more stars are shown in figure 3. Particularly for the fainter stars, the noise in the spectra is not always negligible. The instrumental sensitivity drops a factor of 6 from 1250 to 1180 Å, so that the fits are often poorer in the short-wavelength wing of the absorption profile. Also, the points near line center are less reliable for the distant stars, because the correction for local  $L\alpha$  emission is greatest at  $\lambda_0$ . Some of the prominent lines commonly observed in rocket spectra are indicated at the top of figure 3.

Table 1 summarizes the results for the 10 stars. The spectral types and photometry are from Lesh (1968). The next two columns are the *Mariner 9* values of  $N_H$  and the upper and lower limits to the error bars. The OAO column densities from table 1 of SJ and a few rocket measurements are included for comparison.

#### IV. COMPARISON OF RESULTS

The stars are placed in order of their spectral types in figure 3 to better illustrate how the lines that contaminate the  $L\alpha$  profile change with temperature and luminosity. The N v resonance doublet at 1238.8 and 1242.8 Å is the most troublesome for the hottest stars, while the resonance transition of Si III at 1206.5 Å is strong at B2. Near 1300 Å in figure 3 the Si III multiplet from an excited level (6.6 eV) confirms the increasing importance of Si III from O to B2. The N v line in 15 Mon and  $\xi$  Per is

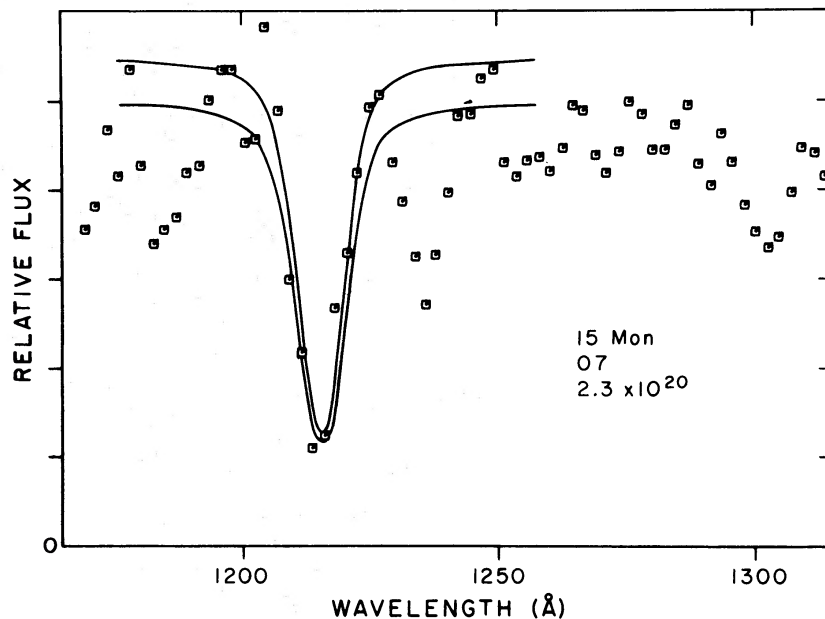


FIG. 2.—Two profiles for  $F_S$  ( $N_H = 2.3 \times 10^{20} \text{ atoms cm}^{-2}$ ) and the second-order spectrum of 15 Mon (O7). The difference of 10 percent in the two continuum levels does not greatly affect the fit at line center but does help in locating the true value of  $F_0$  from the fit in the wings.

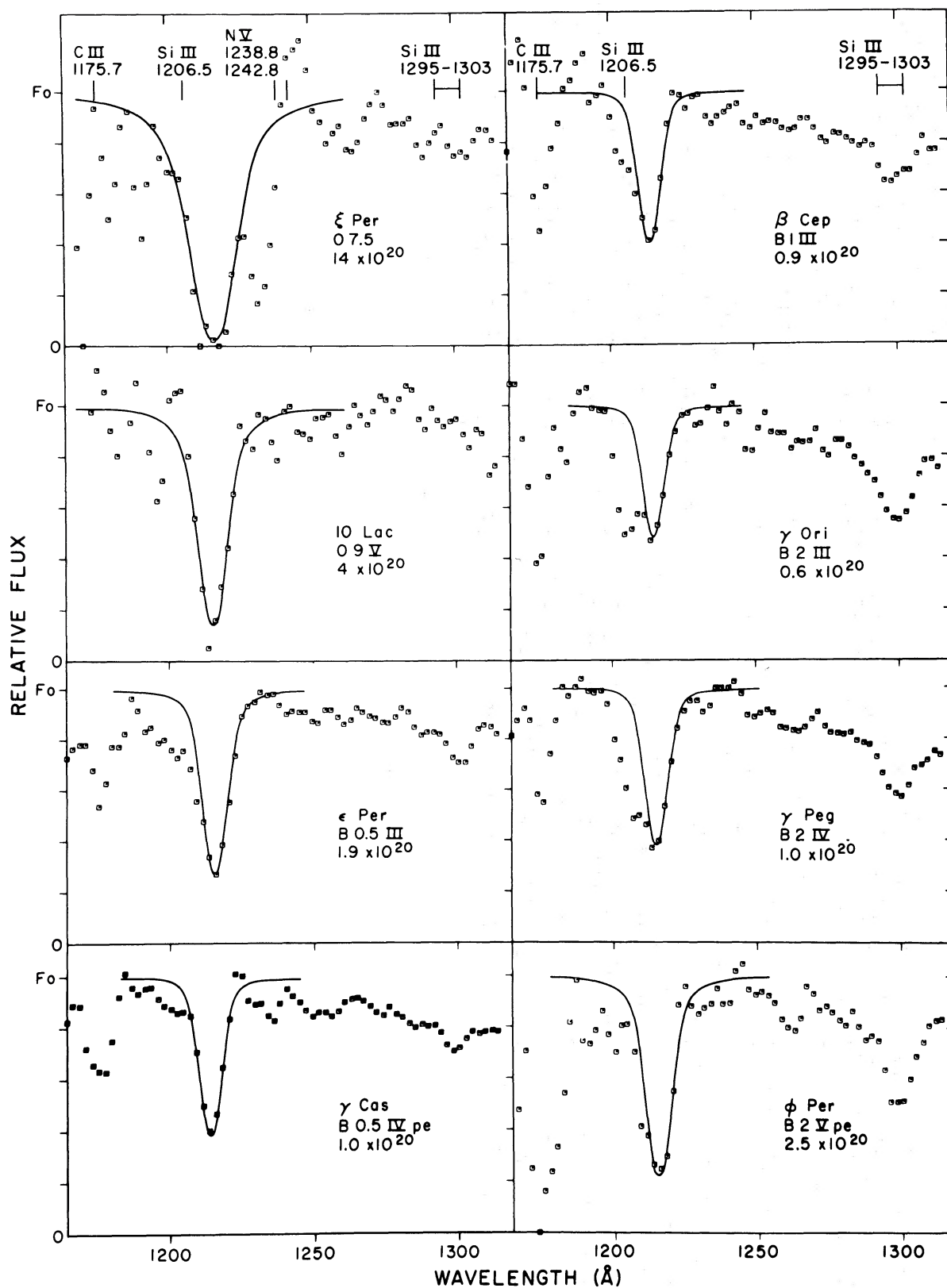


FIG. 3.—Second-order data and best-fit profiles for eight more stars. Laboratory wavelengths for some prominent lines are indicated at the top of the figure. The number below the star name and spectral type is the value of  $N_{\text{H}}$  for the solid curve.

TABLE 1  
SUMMARY OF RESULTS

Name	Spectral Types	$V$	$B - V$	$Mariner N_H$ ( $10^{20} \text{ cm}^{-2}$ )	Error Range ( $10^{20} \text{ cm}^{-2}$ )	OAo $N_H$ ( $10^{20} \text{ cm}^{-2}$ )	Rocket $N_H$ (Ref.) ( $10^{20} \text{ cm}^{-2}$ )
$\gamma$ Peg.....	B2 IV	2.84	-0.23	1.0	0.8-1.5	1.3	
$\zeta$ Cas.....	B2 IV	3.68	-0.20	1.9	1.4-2.6	5.0	
$\gamma$ Cas.....	B0.5 IVpe	2.58	-0.20	1.0	0.7-1.2	1.9	1.0 (1)
$\phi$ Per.....	B2 Vpe	4.09	-0.04	2.5	1.4-4.0	10.	
$\epsilon$ Per.....	B0.5 III	2.90	-0.18	1.9	1.4-2.5	3.0	1.1 (2)
$\xi$ Per.....	O7.5	4.03	+0.01	14.	10.-20.	20.	4.2 (2), 20 (3)
$\gamma$ Ori.....	B2 III	1.64	-0.21	0.6	0.4-0.8	0.65	0.40 (4)
15 Mon....	O7	4.65	-0.25	2.3	1.6-3.0	1.7	
$\beta$ Cep.....	B1 III	3.19	-0.23	0.9	0.7-1.2	1.0	
10 Lac....	O9 V	4.88	-0.20	4.	3.-8.	7.0	

REFERENCES.—(1) Bohlin 1970; (2) Carruthers 1970; (3) Morton, Jenkins, and Macy 1972; (4) Carruthers 1968.

resolved from  $L\alpha$  even though the  $N \text{ v}$  absorption is shifted shortward to 1232.5 Å in  $\xi$  Per. This P Cygni profile with the emission at 1245.5 Å is in agreement with a higher-resolution spectrum of  $\xi$  Per (Morton, Jenkins, and Macy 1972). This line profile is typical for supergiants (Morton, Jenkins, and Bohlin 1968) and substantiates the supergiant classification for  $\xi$  Per of Conti and Alschuler (1971). The prototype stars used by SJ for 15 Mon and  $\xi$  Per are appropriate, and the agreement between UVS and OAO column densities is good. On the other hand, 10 Lac seems to be missing the strong  $N \text{ v}$  absorption present in the prototype  $\zeta$  Oph (O9.5 V). If the lack of a  $N \text{ v}$  line prejudiced the continuum level too high, SJ could have overestimated  $N_H$  for 10 Lac.

A high-resolution spectrum of the B0.5 star  $\gamma$  Cas (Bohlin 1970) does not show as much absorption near  $L\alpha$  as does the prototype star  $\delta$  Sco (B0.5 IV). Again, a small misplacement of the continuum by SJ might explain why the OAO result is almost twice that of the *Mariner* and rocket column densities. The spectrum of  $\epsilon$  Per in figure 3 also shows a lack of absorption in the long-wavelength wing of  $L\alpha$ , so that the differences in the spectra of the prototype and  $\epsilon$  Per may explain the substantial disagreement of the UVS and OAO values of  $N_H$ . The reason for the large discrepancy between the results for  $\zeta$  Cas or  $\phi$  Per is not apparent. Phi Persei is a peculiar star and the C III line is stronger than for the other B2 stars, but this minor spectral difference cannot explain a factor-of-4 difference in the two values of  $N_H$ .

In summary, the *Mariner* column densities are consistently lower than the OAO values with a mean ratio of 0.70. If the 10 stars considered here are typical of the general population, a systematic reduction of the values of SJ is suggested. In any case, the main conclusions of SJ are not affected. They found a large scatter in the correlation between  $N_H$  and 21-cm data but a fair correlation of  $N_H$  with interstellar Na I, Ca II, and color excess. Unfortunately, the present results do not greatly improve the scatter in any of the correlations. The poor comparison between  $L\alpha$  and 21-cm column densities may be caused by large radio beamwidths and suggests that the sky-brightness distribution at 21 cm could be quite lumpy if studied at sufficiently high spatial resolution. The data compiled by SJ are incomplete for the D-lines of Na I. Marschall and Hobbs (1972) recent interferometric scans of the K-line of Ca II include only six of the 10 stars discussed here. More work is needed at 21 cm and in the visual for comparison with the definitive measurements of interstellar absorption lines in the ultraviolet which are expected from OAO-3 (*Copernicus*).

C. A. Barth was principal investigator on the *Mariner 9* ultraviolet spectrometer team. A. L. Lane and M. R. Molnar helped in obtaining and reducing the data. C. F. Lillie provided advice and encouragement. This research was sponsored by the National Aeronautics and Space Administration.

## REFERENCES

- Bertaux, J. L., Ammar, A., and Blamont, J. E. 1972, *Space Res.*, **12**, 1559.  
 Bertaux, J. L., and Blamont, J. E. 1971, *Astr. and Ap.*, **11**, 200.  
 Bohlin, R. C. 1970, *Ap. J.*, **162**, 571.  
 Bohlin, R. C., Henry, R. C., and Swandic, J. R. 1973, *Ap. J.*, **182**, 1.  
 Carruthers, G. R. 1968, *Ap. J.*, **151**, 269.  
 ———. 1970, *Ap. J. (Letters)*, **161**, L81.  
 Conti, P. S., and Alschuler, W. R. 1971, *Ap. J.*, **170**, 325.  
 Jenkins, E. B. 1970, in *Ultraviolet Stellar Spectra and Related Ground-Based Observations* (IAU Symposium No. 36), ed. L. Houziaux and H. E. Butler (Dordrecht: Reidel Publishing Co.), p. 281.  
 ———. 1971, *Ap. J.*, **169**, 25.  
 Kerr, F. J., and Westerhout, G. 1965, in *Stars and Stellar Systems*, Vol. 5, *Galactic Structure*, ed. A. Blaauw and M. Schmidt (Chicago: University of Chicago Press), p. 167.  
 Kovach, W. S. 1972, *Ap. J.*, **173**, 287.  
 Lesh, J. R. 1968, *Ap. J. Suppl.*, **16**, 371.  
 Lillie, C. F., Bohlin, R. C., Molnar, M. R., Barth, C. A., and Lane, A. L. 1972, *Science*, **175**, 321.  
 Marschall, L. A., and Hobbs, L. M. 1972, *Ap. J.*, **173**, 43.  
 Morton, D. C., Jenkins, E. B., and Bohlin, R. C. 1968, *Ap. J.*, **154**, 661.  
 Morton, D. C., Jenkins, E. B., and Macy, W. W. 1972, *Ap. J.*, **177**, 235.  
 Pearce, J. B., Gause, K. A., Mackey, E. F., Kelly, K. K., Fastie, W. G., and Barth, C. A. 1971, *Appl. Opt.*, **10**, 805.  
 Savage, B. D., and Jenkins, E. B. 1972, *Ap. J.*, **172**, 491.  
 Thomas, G. E., and Krassa, R. F. 1971, *Astr. and Ap.*, **11**, 218.